Nonlinear response of RC frame-wall structures

A.A.Hashish & H.M.Aktan
Wayne State University, Detroit, Mich., USA

ABSTRACT: This paper describes an analytical procedure and presents a computer program for predicting the static and/or dynamic nonlinear response of RC frame-wall structures. The stiffness characteristics of reinforced concrete are modeled for three states representing uncracked, cracked and strain-hardening under flexural and shear deformations. The structure is idealized by line elements representing beams and columns and a two-dimensional element representing the structural wall elements. The accuracy of the proposed model and the analytical procedure are demonstrated by comparisons with the experimental and the previous analytical responses of an RC portal frame building reported in the literature.

1 INTRODUCTION

The nonlinear analysis of RC buildings has been the subject of considerable research during the last decade [Keshavarzian 1984 and Meyer et al. 1983]. However, recent experimental research on full-scale and large-scale buildings [Aktan and Bertero 1984] has indicated that the currently-used analytical models and, consequently, the related computer programs, lead to significant inconsistencies between predicted and measured responses. The lack of correlation between the analytical and the experimental results is primarily due to the inadequacy of realistic idealizations of the RC element behavior states, e.g., the neglect of the cracking behavior state of, in particular, the wall elements. Studies have indicated that a proper idealization of the behavior of RC elements and, consequently, reliable estimates of the stiffness, strength and damping characteristics are prerequisites for reliable nonlinear response analysis.

Previous models are commonly grouped based on two different concepts with respect to how the nonlinearities are distributed within the element. The first group is based on the plastic hinge concept and assumes that the nonlinearities are confined to two points at the member ends; these are commonly modeled as nonlinear rotational springs. The second group is based on the finite regions concept, which assumes that the nonlinearities are distributed along a portion of the length of the element.

The plastic hinge concept is further subcategorized as the "One-Component Model" and the "Two-Component Model." In the "One-Component Model" [Otani 1972 and Giberson 1967], the element clear span consists of an elastic element with one equivalent nonlinear rotational spring attached at each end. In the "Two-Component Model" [Mahin and Bertero 1975], the element consists of an elastic component and an elasto-plastic component which develops a plastic hinge at either end when the moment exceeds a specified yielding value. The shear behavior in the plastic hinge concept is modeled much in the same manner as for flexural modeling by considering plastic shear distortions of the hinges at the member ends. The hypothesis of the plastic hinge concept is not capable of adequate representation of the RC element behavior because the resulting element stiffness matrix is constant in yielding independently of the severity of yielding due to all of the inelastic actions being confined to the rotational hinges. In addition, the "Two-Component Model" does not relate to the physical behavior of the element.

The finite regions concept overcomes some of these shortcomings by taking the finite size of the plastic regions into consideration. The finite regions concept is subgrouped as the "Multiple Spring Model" and the "Finite Plastic Regions

Model." In the "Multiple Spring Model" [Keshavarzian 1984], the element is divided into several subelements represented in the form of a sequence of nonlinear rotational springs connected in series. The disadvantages of the "Multiple Spring Model" are in principle similar to those of the "Plastic Hinges Model." In the "Finite Plastic Regions Model" [Keshavarzian 1984 and Meyer et al. 1983], the element clear span is considered to consist of two zone types: an elastic central zone and two variable-length inelastic zones located at each end of the element. The shear modeling in the "Finite Plastic Regions Concept" is such that the inelastic values of shear rigidities in the inelastic zones are reduced in direct proportion to the flexural rigidities. The shortcoming of the "Finite Plastic Regions Model" is that the flexural rigidities of the plastic regions are evaluated at the element ends and are assumed to remain constant throughout the length of the plastic zones and are therefore not adequately represented. Furthermore, none of the models considers the cracking behavior state.

The proposed model is an improvement on the "Finite Plastic Regions Model" [Hashish, 1987]. The improvements include:

1. Incorporation of the third behavior state for cracking prior to yielding.
2. Evaluation of flexural rigidities of the inelastic zones based on the moment and curvatures state at the middle of each zone.
3. Incorporation of an idealization for shear rigidity in the cracking and strain-hardening states.

The primary objective of this paper is to describe the proposed analytical model. The analysis procedure and the accuracy of the model will be demonstrated by comparisons between the experimental and the predicted responses for a single-bay one-story frame [Gulkan and Sozen 1971 and Meyer et al. 1983].

2 THE PROPOSED MODEL

In this study, the analytical model of an RC building is based on the assumptions that:

1. The building consists of a group of planar frames connected in parallel. Frames consist of line elements for stiffness calculation purposes; however, the effect of wall rocking on the floor beams is included.
2. The line elements are idealized by five variable-length subelements connected in series representing RC behavior states as uncracked, cracked and strain-hardening.

In the proposed model, termed the "Five Variable-Length Subelement Model," the RC element chord zone or clear span consists of five zones in three behavior states, the uncracked or elastic, cracked, and strain-hardening. The two strain-hardening and cracked zones are adjacent to each end and the middle zone remains as uncracked or elastic. The representation of behavior zones in a typical RC element is shown in fig.2.1. Inelastic actions, defined in a set of idealized hysteresis rules, are confined to the four cracked and strain-hardening zones. The subelement lengths and flexural and shear rigidities are updated after each load or time increment for the current element stiffness matrix calculations.

2.1 Subelement lengths

The current subelement lengths are calculated from the linear bending moment variation along the element, based on the current cracked and yielding moment capacities of the cross-section. The cracking and yielding moment capacities are updated at each load or time increment by incorporating the effect of axial force-moment interaction with the current axial force. The current subelement lengths are calculated from a linear moment variation along the element, that assuming the total accumulated length of the inelastic zones at each end is non-decreasing. The subelement lengths are calculated at any time or load increment, as shown in figure 2.1.

2.2 Flexural rigidity

The flexural rigidity of an RC element is described by the moment-curvature relationship through a set of idealized hysteresis rules. The moment-curvature relationship for an RC element is evaluated based on the following assumptions:

1. The Bernoulli-Euler assumption of linear strain distribution along the depth of a section.
2. Hognestad's proposed model as modified by Kaba and Mahin (1983) for the stress-strain relationship for concrete in compression (fig.2.2a).
3. A proposed model for the stress-strain relationship for concrete in tension [Hashish 1987] (fig.2.2b).
4. A piecewise linear stress-strain relationship for reinforcing steel (fig.2.2c).

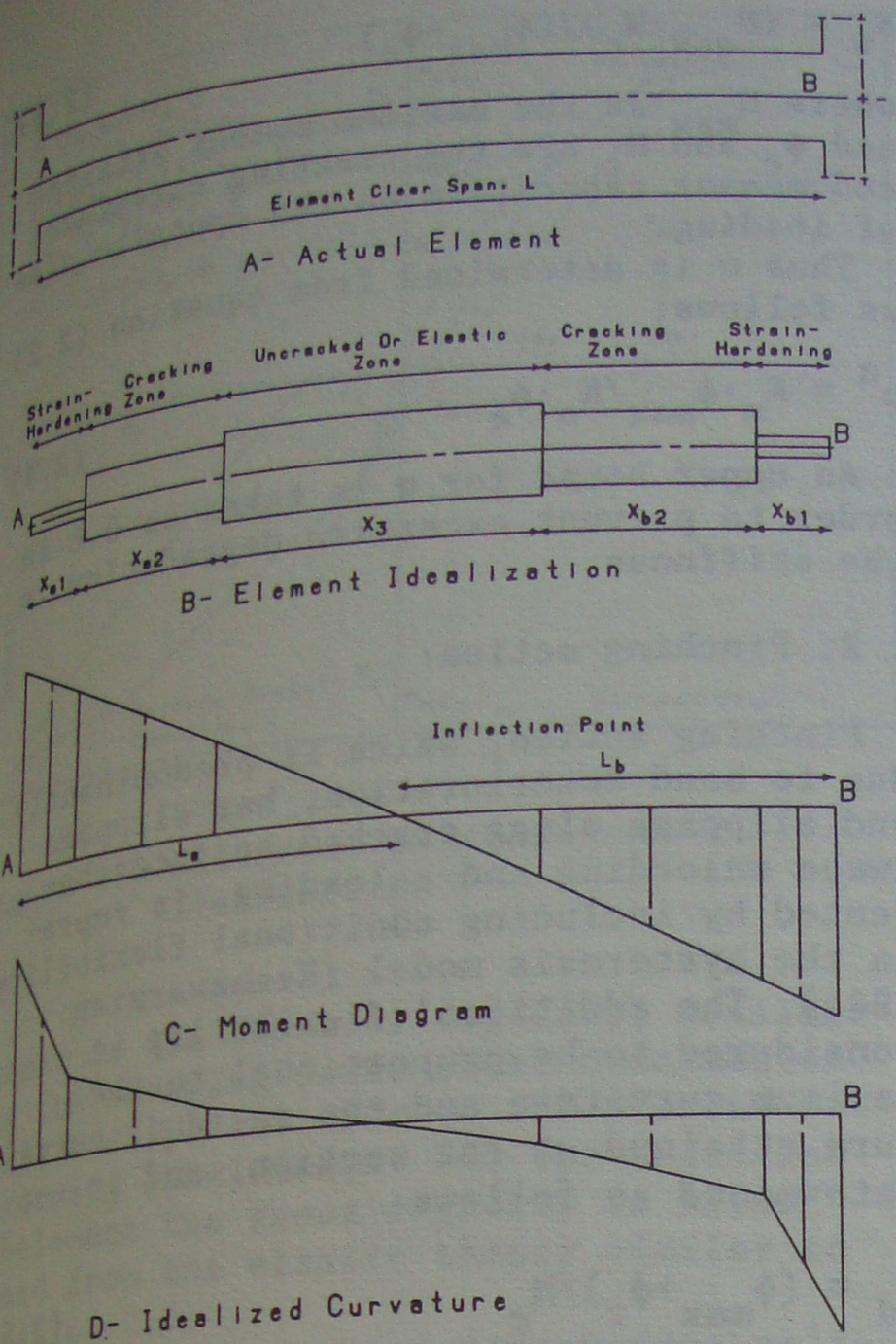

Figure 2.1 Five variable-length subelements model

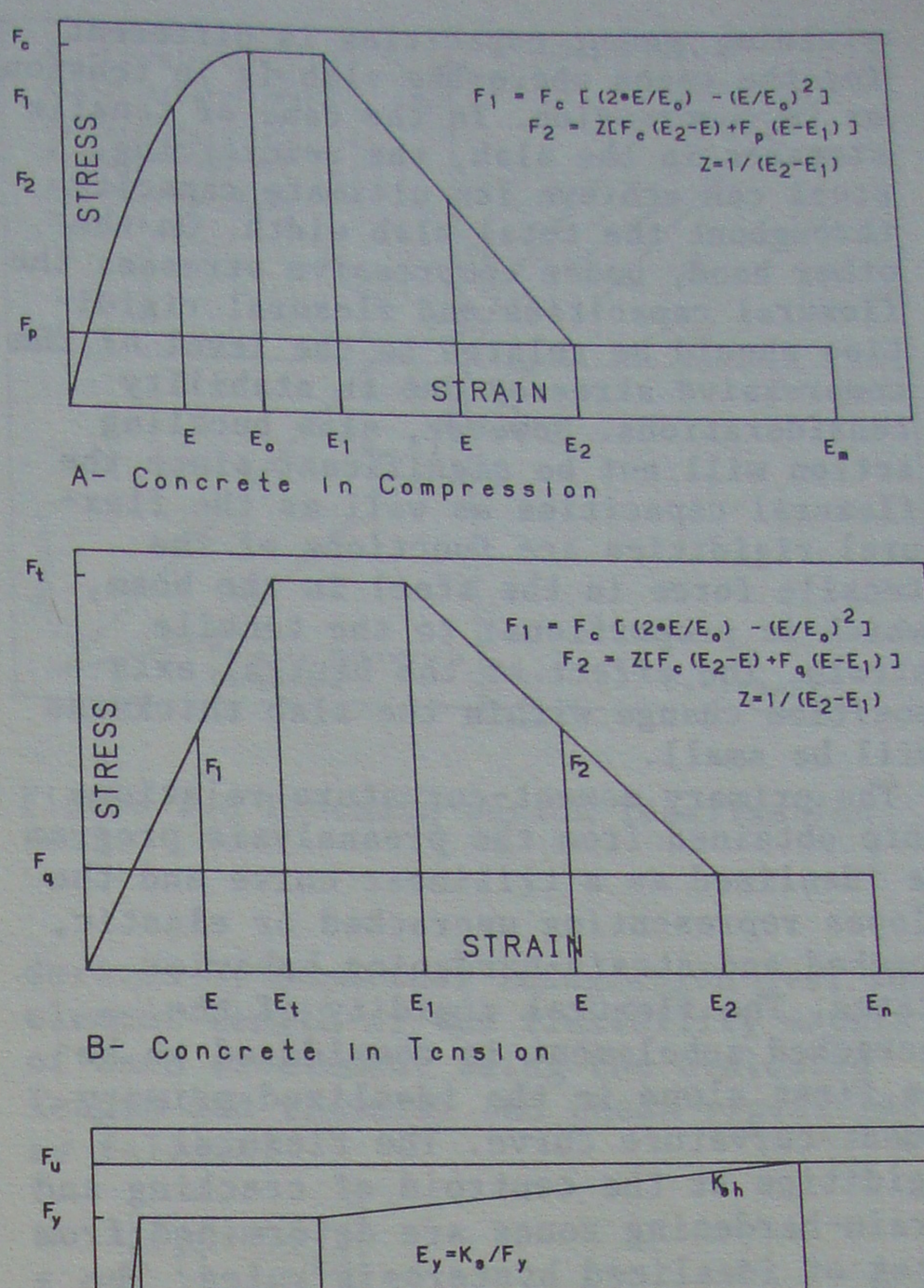

Figure 2.2 Stress-strain relationship

5. The flexural rigidities and flexural capacities of a section are assumed to be a function of both curvature and axial force. The effect of the axial force-flexure interaction on the moment-curvature relationship is determined as follows:

$$M = f(\phi, P) \tag{2.1a}$$

$$\frac{dM}{d\phi} = \frac{\partial F}{\partial \phi} + \frac{\partial F}{\partial P} \cdot \frac{\partial P}{\partial \phi} \tag{2.1b}$$

where M and ϕ are moment and curvature of a section, P is axial force and F is the moment function.

For the evaluation of flexural rigidity, the analysis requires the determination of the primary moment-curvature relationship. A computer program for preanalysis [Hashish 1987] is utilized in obtaining the axial force-cracking moment and axial force-yielding moment interaction relations. The primary moment-curvature curve and axial force-cracking moment and axial force-yielding moment interaction relations are investigated for various elements with beam slab T-sections, shear wall barbell sections, and rectangular sections. The following generalizations are incorporated into the response analysis program based on the results obtained from the preanalysis:

1. The cracking moment capacity for a structural wall section is on the order of 45-55% of the yielding moment capacity, and consequently the cracked behavior state must be incorporated into the analysis.

2. The cracking and yielding moment capacities are assumed to be linearily proportional to the level of axial force in the element below the balanced point.

3. The contribution of slab width to the beam flexural rigidity and cracking and

yielding moment capacities is different for the cases where the slab is in tension or in compression. In the case of tensile stresses in the slab, the reinforcing steel can achieve its ultimate capacity throughout the total slab width. On the other hand, under compressive stresses the flexural capacities and flexural rigidities should be related to the level of the compressive stresses due to stability considerations. However, slab buckling action will not be significant since the flexural capacities as well as the flexural rigidities are functions of the tensile force in the steel in the beam, which is proportional to the tensile strain. The effect of the neutral axis position change within the slab thickness will be small.

The primary moment-curvature relationship obtained from the preanalysis program is idealized as a trilinear curve and the slopes representing uncracked or elastic, cracked and strain-hardening behavior states. The flexural rigidity of the uncracked subelement is considered to be the first slope in the idealized primary moment-curvature curve. The flexural rigidities at the centroid of cracking and strain-hardening zones are determined from a set of idealized hysteresis rules. The flexural rigidity of the centroid section is assumed to remain constant along the length of each zone.

The idealized hysteresis rules used in the analysis are a modification of Takeda-type (1971) hysteretic moment-curvature behavior. The modificatons to the Takeda hysteresis rules are:

1. The unloading stiffness:

The unloading stiffness is considered by Takeda and others to be in the form:

$$K_u = K_o \cdot (\phi_e/\phi_{max})^{\alpha} \qquad (2.2)$$

where K_u is the unloading stiffness, K_o is the elastic or equivalent elastic stiffness, ϕ_e is either the cracking or yielding curvature depending on the maximum curvature ϕ_{max} attained, and α is an exponent ($0.0<\alpha<0.5$ or 0.6). Strictly speaking, unloading should be referred to a fixed point on the primary moment curvature for adequate representation of the degradation level. The fixed point is considered to be the point defined by cracking moment and curvature on the opposite side of the primary moment curvature, as shown in figure 2.3. The unloading stiffness is then determined from the relation:

$$K_u = (M_{max}-M_c)/(\phi_{max}-\phi_c) \qquad (2.3)$$

where M_{max} is the maximum moment attained and ϕ_c and M_c are the cracking curvature and moment capacities on the opposite side of loading.

Thus α is determined from equation (2.2) as follows:

$$e^{\alpha} = K_u \cdot \phi_{max}/K_o \cdot \phi_e \qquad (2.4)$$

An upper bound for α is taken as 0.6 in order to prevent excessive degradation in the stiffness.

2. Pinching action:

Pinching action, which is predominantly due to bond deterioration, bar slippage and slippage along cracked surfaces between unloading and reloading, is represented by including additional flexibility in the hysteresis model (Keshavarzian 1984). The additional flexibility is considered to be proportional to the maximum curvature and the residual curvature attained at the section, and is determined as follows:

$$F_d = (\phi_{max}+\phi_r)/M_e \qquad (2.5)$$

where F_d is the additional flexibility, ϕ_r and ϕ_{max} are the residual and maximum attained curvature, and M_e is either the cracking or yielding moment curvature, depending on the attained maximum curvature. A representation of pinching actions is illustrated in figure 2.4.

2.3 Shear rigidity

Shear rigidity is described separately for RC prismatic members (beams and columns) and the structural wall elements. For prismatic members the shear deformation is considered to be secondary to the total deformation, where flexural deformation is dominant. The inelastic shear rigidity for cracked and strain-hardening subelements is considered to be proportional to the flexural rigidities by applying the elastic theory at each behavior state to the subelement as follows:

$$GA_i = EI_i \cdot A_o/[2I_o(1+\mu_i)] \qquad (2.6)$$

where GA_i, EI_i and μ_i are shear and flexural rigidities and poission's ratio of subelement i, and A_o and I_o are the gross area and initial moment of inertia of the section. For wall elements in which the shear deformation is significant, the shear rigidity is described in a similar

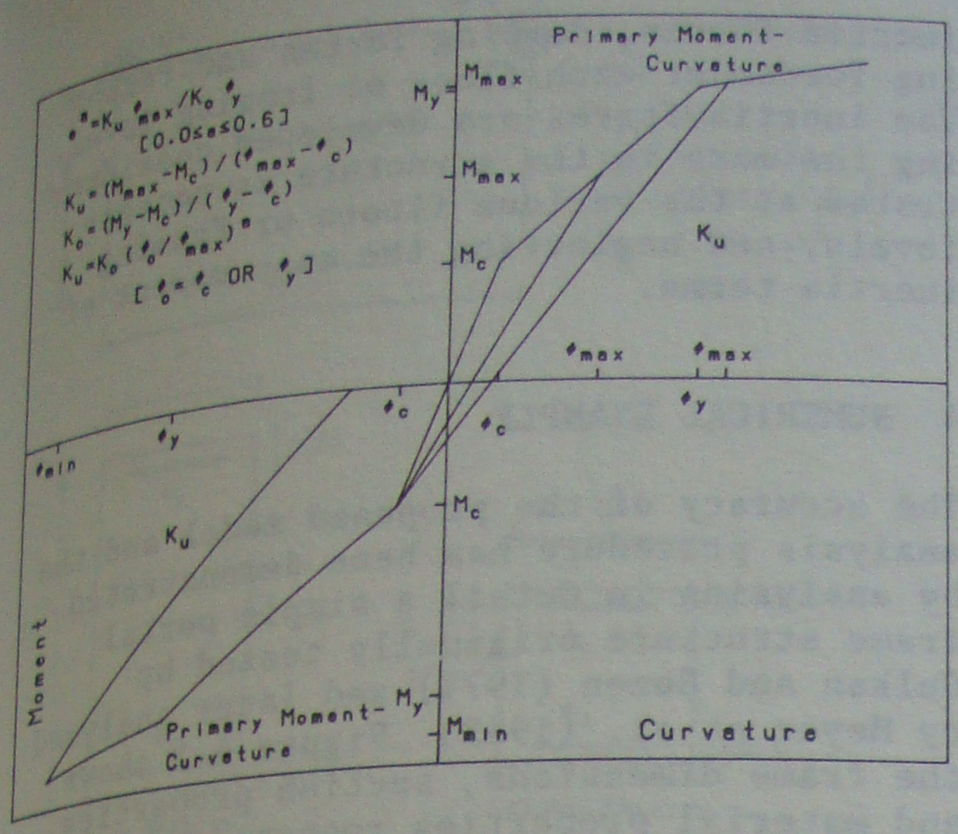

Figure 2.3 Stiffness degredation idealization

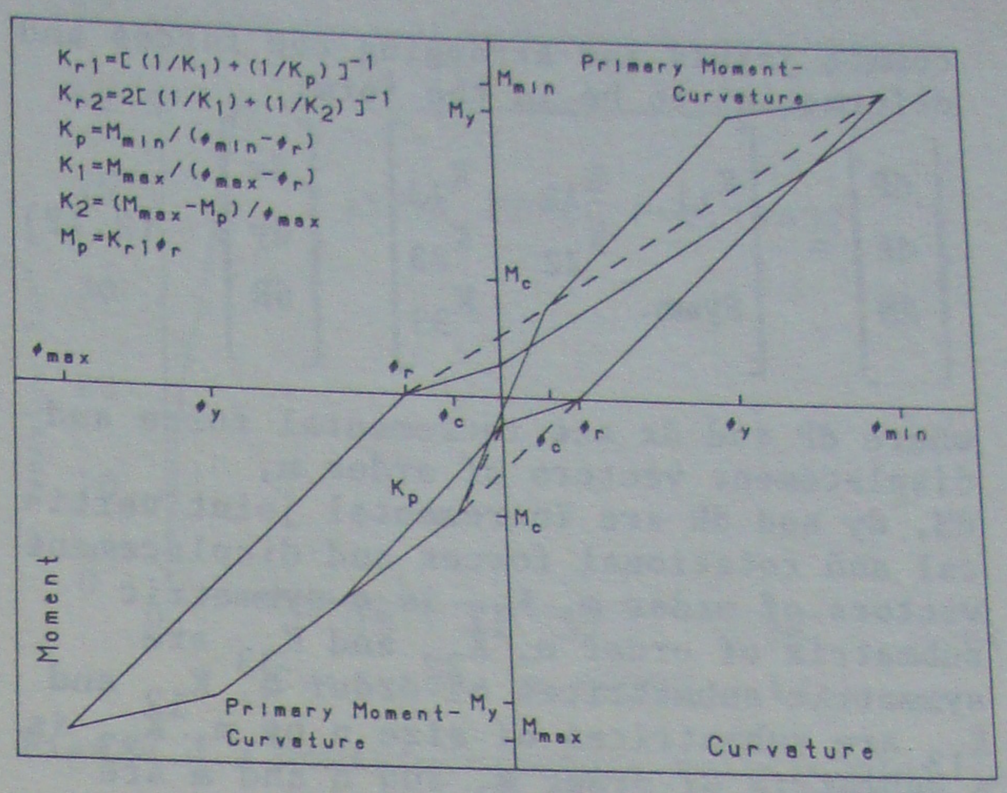

Figure 2.4 Pinching action idealization

manner as the flexural rigidity, considering the shearing force-shear deformation relationships for cracked and strain-hardening subelements. For the uncracked subelement the shear rigidity is determined from the elastic theory similar to equation 2.6.

The shear force-shear deformation relationship is evaluated for cracked zones based on the aggregate interlock and dowel action mechanism, while for the strain-hardening subelements the relationship is evaluated based on the aggregate interlock mechanism only. The effect of the dowel mechanism is not considered in the strain-hardening behavior state because the rigidity of the tensile reinforcement in yielding is small. The shearing force-shearing deformation relationship is derived for the strain-hardening subelements for a section under a progressively increasing shearing force with a constant moment M_o equal to M_y, while for the cracked subelement the shear force-shear deformation relationship is derived for a section under a progressively increasing shearing force with a constant moment M_o as:

$$M_o = (M_y + M_c)/2 \qquad (2.7)$$

where M_y and M_c are the yielding and cracking moment of the cross section respectively.

2.4 Stiffness matrix formulation

The element flexibility matrix for the "Five Variable-Length Subelement Model" is derived by numerical integration over the element length of the flexibility matrix of each subelement using the evaluated length and flexural and shear rigidities as follows:

$$f = \begin{bmatrix} f_{11} & f_{12} \\ f_{12} & f_{22} \end{bmatrix} \qquad (2.8)$$

where

$$f_{11} = \sum_{i=1}^{5} \frac{L_i}{GA_i L^2} + \frac{B_i^3 - A_i^3}{3L^2 \cdot EI_i} \qquad (2.9)$$

$$f_{12} = \sum_{i=1}^{5} \frac{L_i}{GA_i L^2} + \frac{B_i^3 - A_i^3}{3L^2 EI_i} - \frac{B_i^2 - A_i^2}{2LEI_i} \qquad (2.10)$$

$$f_{22} = \sum_{i=1}^{5} \frac{L_i}{GA_i L^2} + \frac{(B_i - L)^3 - (A_i - L)^3}{3L^2 EI_i} \qquad (2.11)$$

where L_i is the length of subelement i, EI_i and GA_i are current flexural and shear rigidities, and A_i is the distance between the right end of subelement i and the right end of the element and $B_i = L_i + A_i$.

The current local and global element stiffness matrices are obtained by inverting the flexibility matrix, including the rigid end effects, if any, incorporating the axial force displacement relationship, and introducing the transformation matrix for global coordinates following standard methods of structural analysis. The structural tangent stiffness matrix of the entire frame is formulated by summing all element stiffness matrices at the

common joints and arranging the forces and deformation to be in the form:

$$\begin{Bmatrix} dP \\ dF \\ dM \end{Bmatrix} = \begin{bmatrix} K_{11} & K_{12} & K_{13} \\ & K_{22} & K_{23} \\ \text{Symm.} & & K_{33} \end{bmatrix} \begin{Bmatrix} dx \\ dy \\ dR \end{Bmatrix} \qquad (2.12)$$

where dP and dx are incremental force and displacement vectors of order n, dM, dy and dR are incremental joint vertical and rotational forces and displacement vectors of order m, K_{11} is a symmetric submatrix of order n, K_{22} and K_{33} are symmetric submatrices of order m, K_{12} and K_{13} are submatrices of size n by m, K_{23} is a submatrix of order m, and n and m are the number of stories and number of joints in a frame.

Based on the required type of analysis, the appropriate static condensation procedure is applied to eliminate the undesired degrees of freedom.

3 ANALYSIS PROCEDURE

The options of the analysis procedure are static and/or dynamic response analysis of the frame-wall structure. The static analysis provides the response due to gravity loads and/or quasistatically applied lateral loads. The gravity load analysis is performed to determine the axial force within each element (beam, column and wall) of the structure before performing the dynamic or quasi-static lateral load analysis. From the quasistatically applied lateral loads, analysis is performed to determine the lateral force-displacement relationships.

In the gravity load analysis, the lateral and vertical degrees of freedom are reduced by the static condensation procedure and the equilibrium equation will be :

$$M = K^{*} \cdot R \qquad (3.1)$$

In incremental lateral load analysis the rotational and vertical degrees of freedom are reduced and the equilibrium equation will be:

$$P = K^{*} \cdot X \qquad (3.2)$$

where K^{*} is the condensed stiffness matrix. The dynamic analysis provides the response analysis for harmonic loading and/or seismic ground acceleration. In the dynamic analysis, the equations of motion of a structure are expressed by the equilibrium conditions existing between the inertia forces, damping forces and restoring forces at each floor or framing level. The inertia forces are developed considering the mass in the structure as concentrated at the various floors or framing levels, and neglecting the mass moment of inertia terms.

4 NUMERICAL EXAMPLE

The accuracy of the proposed model and the analysis procedure has been demonstrated by analyzing in detail a simple portal frame structure originally tested by Gulkan and Sozen (1971) and later analyzed by Meyer et al. (1983). Figure 4.1 shows the frame dimensions, section properties, and material properties reported by Meyer (1983). The frame is analyzed for the following three loading cases:

1. Gravity load.
2. Monotonically increasing quasi-static lateral load applied at the top.
3. Four complete cycles of quasi-static lateral load reversals applied at the top.

The gravity load analysis is performed using the cross-sectional properties to determine the axial force within each member. The primary moment-curvature relationship for a member under a constant axial force, the axial force-cracking moment, and the axial force yielding moment interactions are derived for column and beam cross-sections using the pre-analysis program (figures 4.2 and 4.3). The relations obtained for moment-curvature and axial force-cracking moment and axial force-yielding moment interactions are utilized to determine the cracking and yielding moment capacities (for positive and negative direction if different) and the uncracked, cracked and strain-hardening slopes of the idealized primary moment-curvature relation, as well as the rate of change of cracking and yielding moment capacities with the change of axial force (from the axial force-moment interaction relations), as shown in Table 4.1.

Based on the cross-sectional properties obtained from the pre-analysis program, the lateral force-displacement for incremental monotonic and quasistatic cyclic loading and moment curvature relations at the element ends and middle of strain-hardening and cracking susblements is obtained from the response analysis of the portal frame.

It is apparent from the force displacement relationship in figure 4.4 that the proposed analytical model is in better agreement with the experimental results reported by Sozen [1971] than the analytical model proposed by Meter [1983]. The

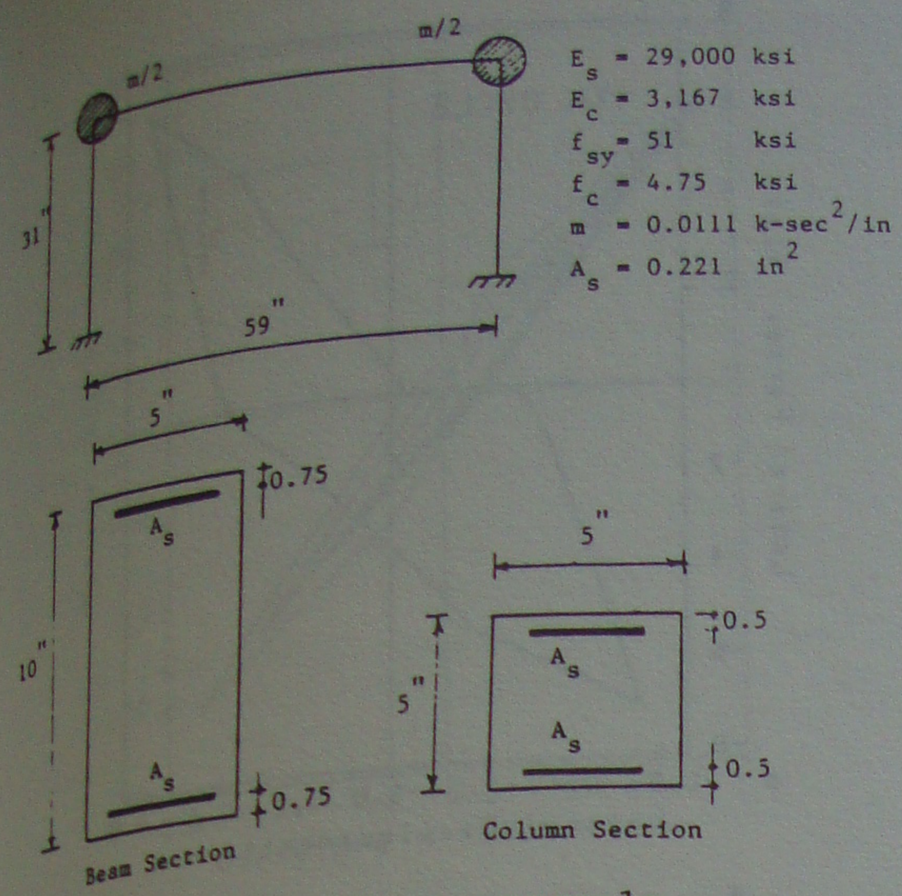

Figure 4.1 Portal frame example

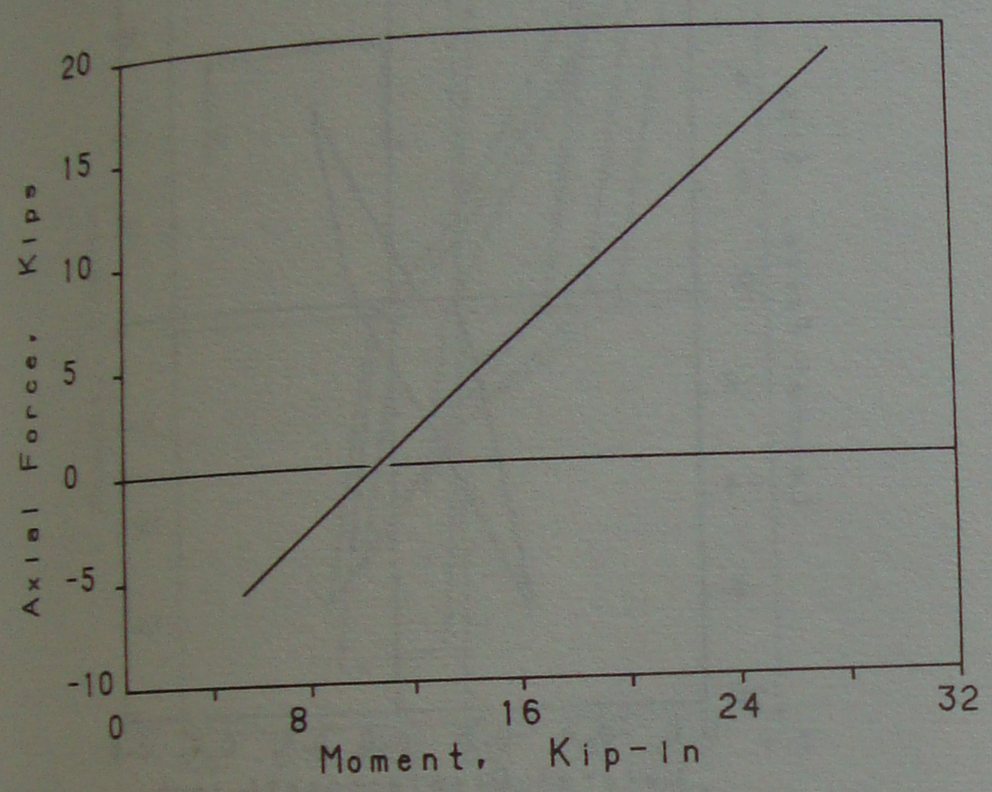

a. Axial force-cracking moment

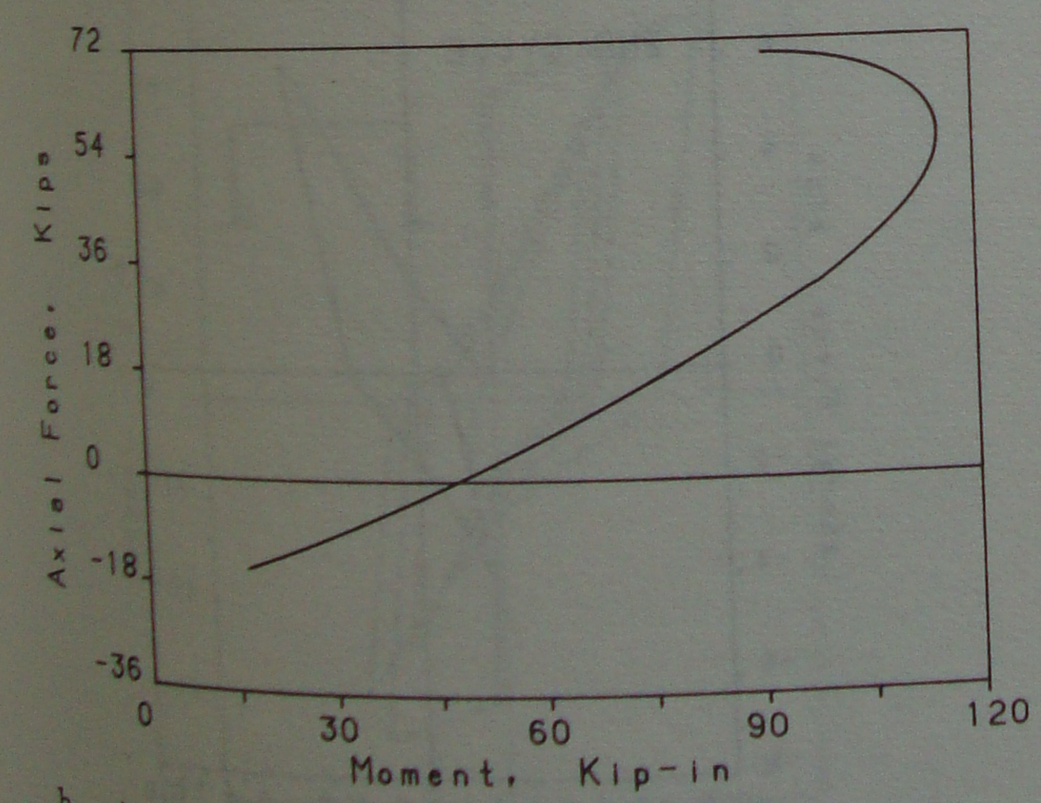

b. Axial force-yielding moment

Figure 4.2 Axial force-moment interaction for column section

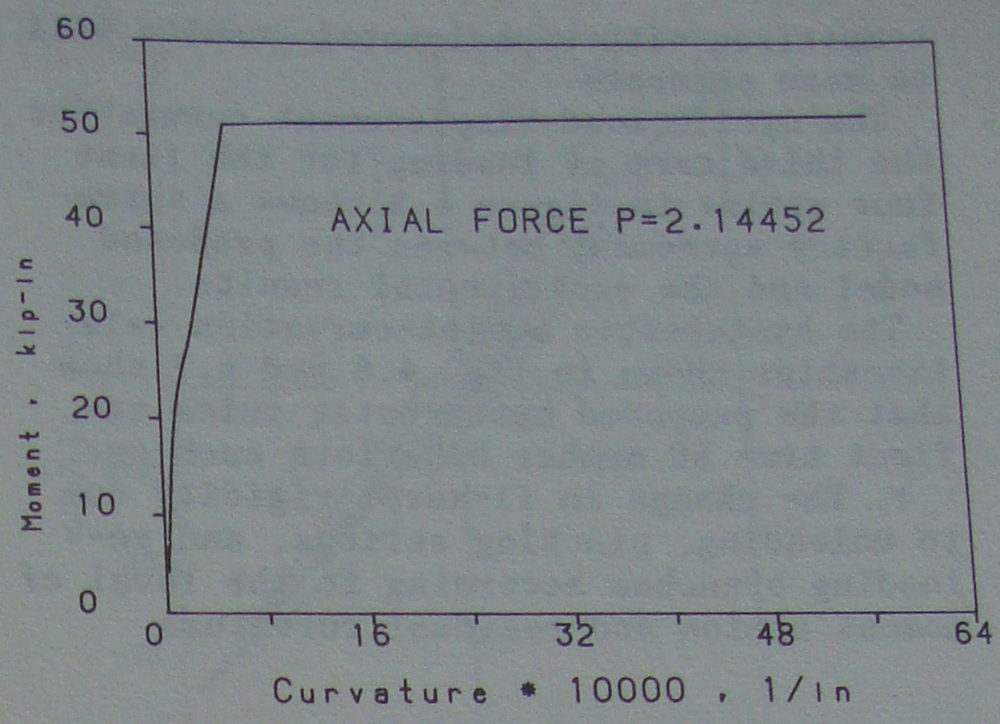

Figure 4.3 Moment-curvature relationship for column section

Table 4.1 Section properties

Parameter	Column	Beam
Cracking moment*	48.0	34.0
Yielding moment	11.0	93.0
Gravity axial load	2.15	-0.21
Uncracked flexural rigidity	1.65×10^5	13.20×10^5
Cracked flexural rigidity	8.61×10^4	31.77×10^4
Strain-hardening flexural rigidity	8.61×10^2	31.77×10^2
$\partial Mc/\partial P$	0.91	1.37
$\partial My/\partial P$	1.85	3.94

*All units are Kips, Kip-inch, and Kip-in^2.

following points are significant in the experimental analytical comparisons:

1. The proposed model accurately describes the decrease in structural stiffness after cracking.
2. The stiffness of the structure after cracking is somewhat higher in the proposed model than that obtained from the test and the previous proposed model.

However, the model proposed by Meyer assumes that every member is fully cracked, and obtains an average stiffness for the uncracked and cracked states. In the proposed model the length of the uncracked zone decreases progressively with increasing loading, and therefore describes the behavior realistically. It is anticipated that with the inclusion of inelastic shear in the proposed model the

comparison with experimental results will be more accurate.

The cyclic load-displacement curves for the third case of loading for the first four cycles in figure 4.5 shows a satisfactory agreement between the proposed model and the experimental results.

The hysterestic moment-curvation relationships shown in fig. 4.6 and 4.7 show that the proposed hysterestic rules reflect true RC member behaviors such as:

1. The change in flexural rigidity due to unloading, pinching actions, and reloading branches according to the level of moment action and residual curvature.

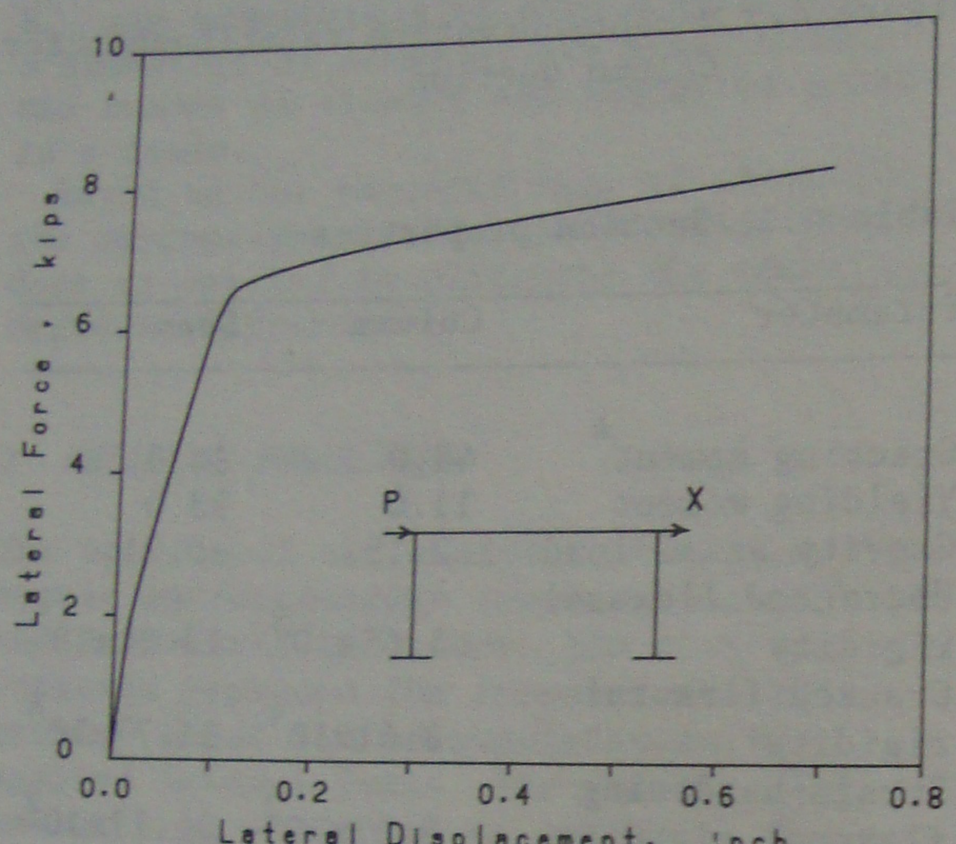

Figure 4.4 Lateral force-displacement relationship

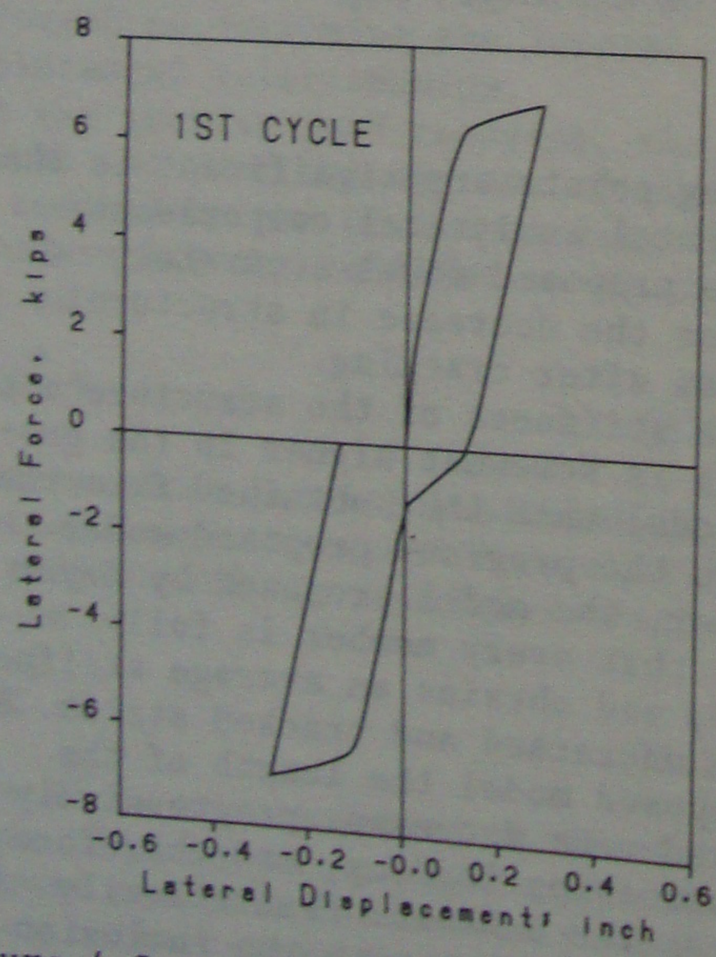

Figure 4.5a Lateral force-displacement relationship for 1st cycle

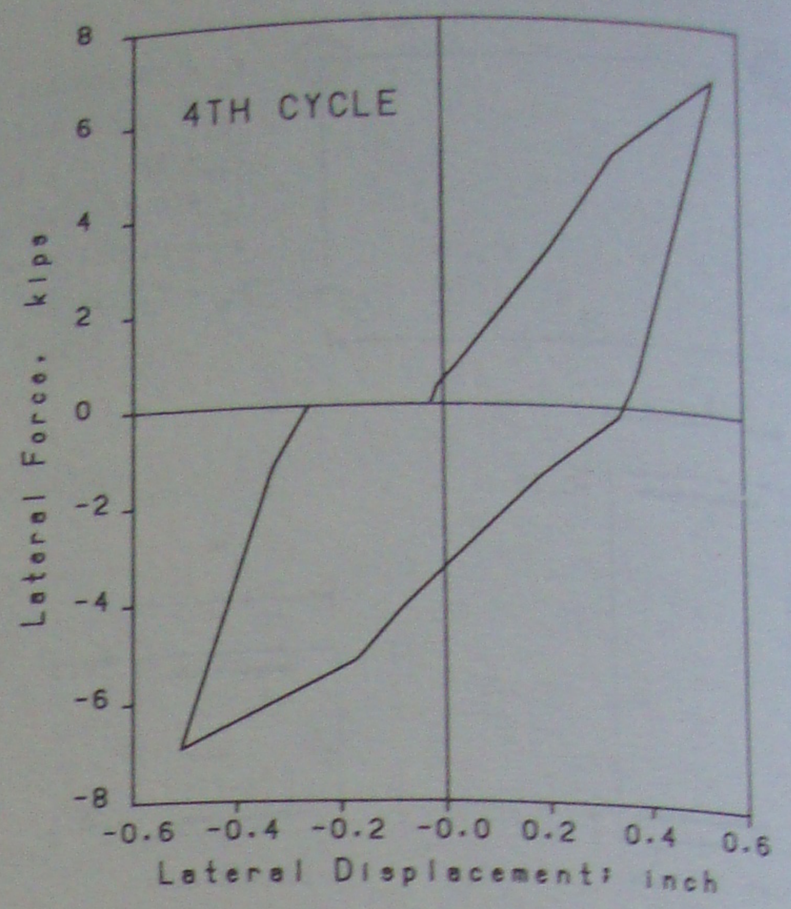

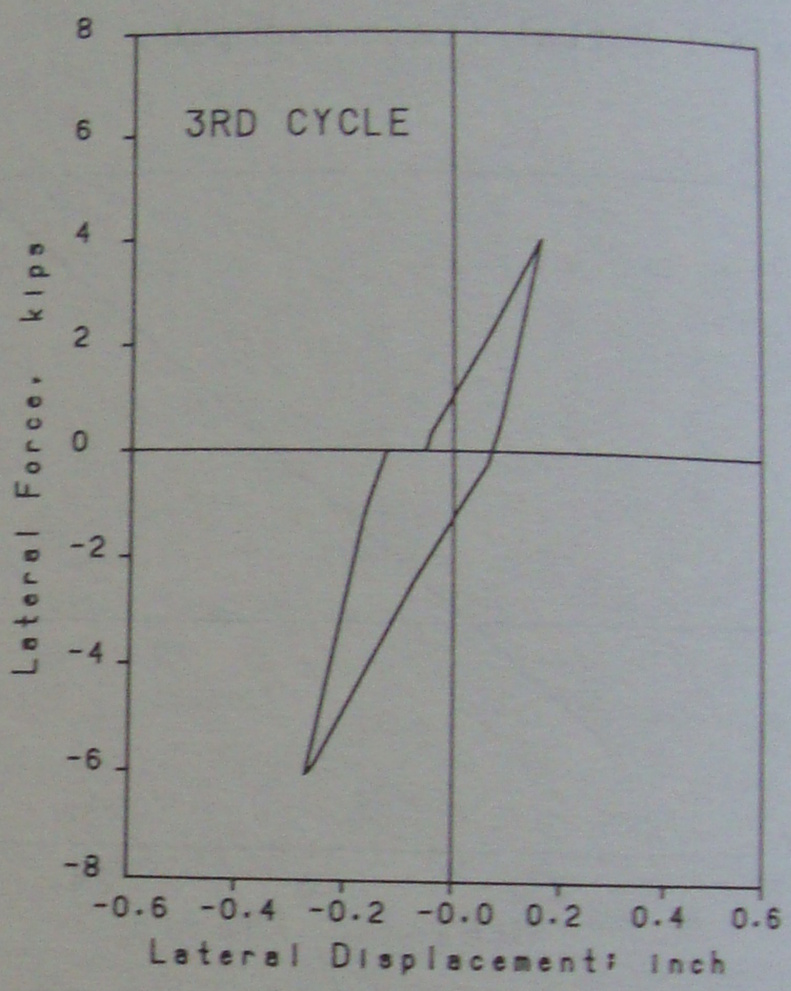

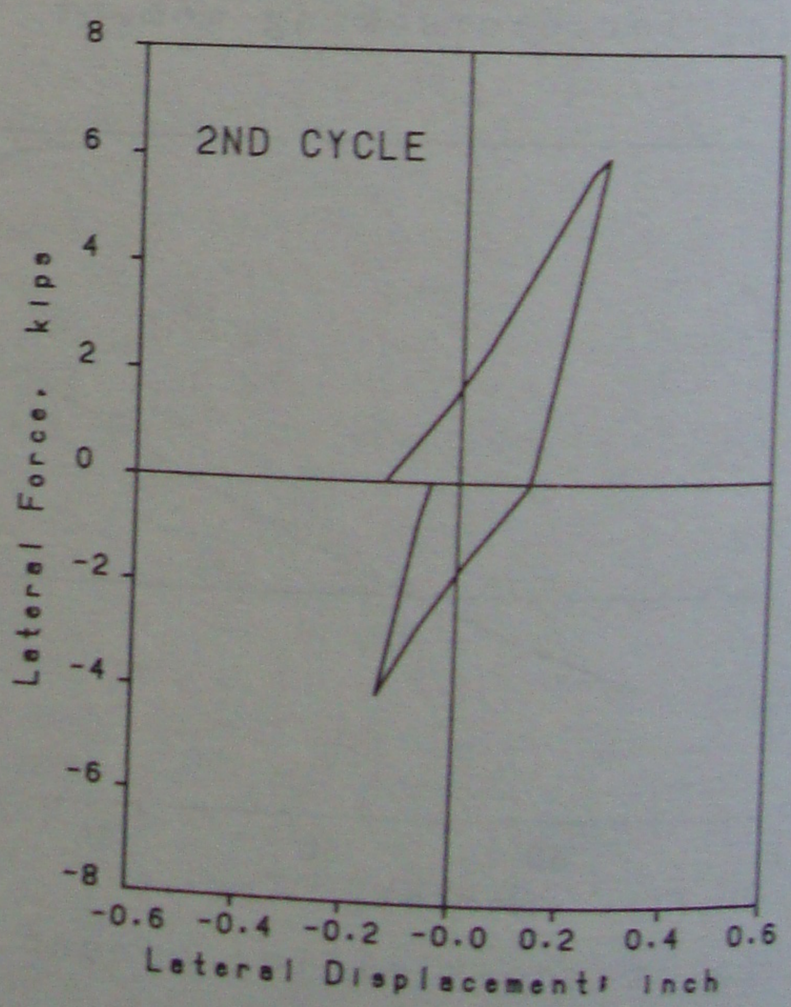

Figure 4.5b-d Lateral force-displacement relationship for the 2nd-4th cycles

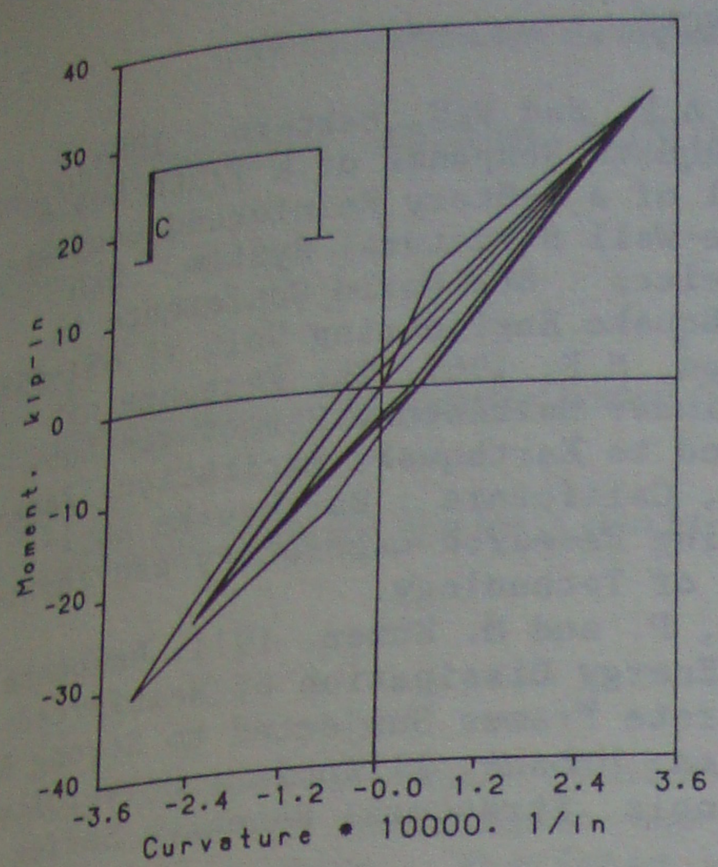

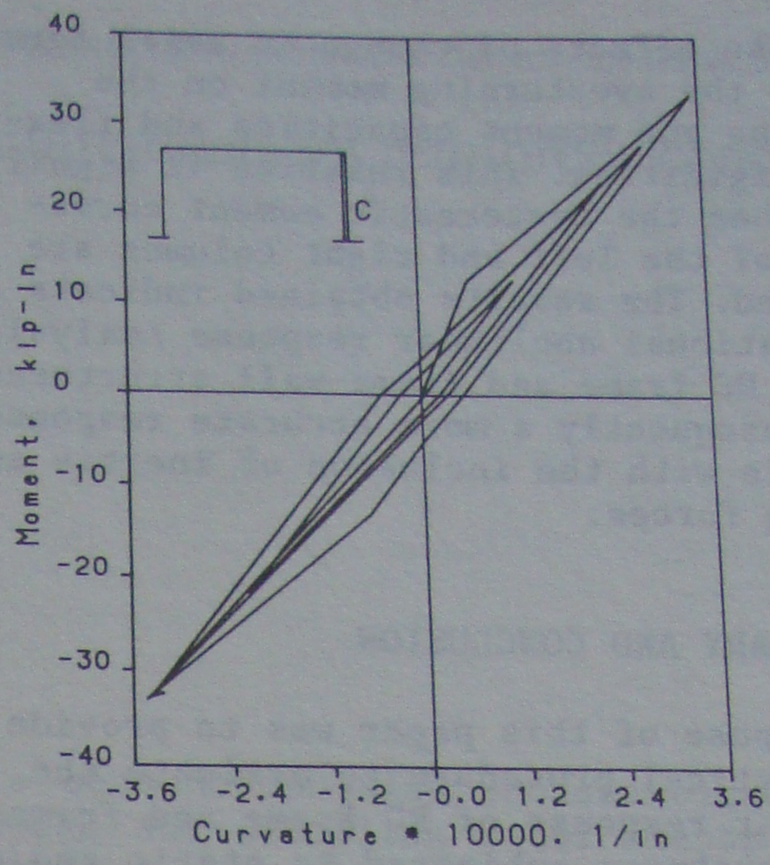

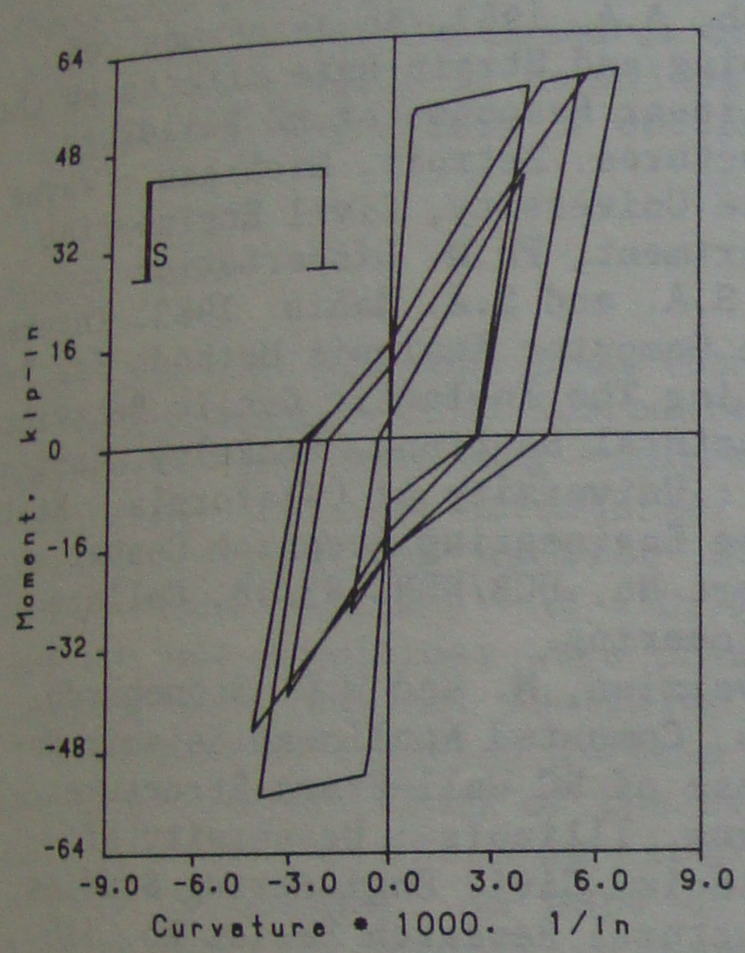

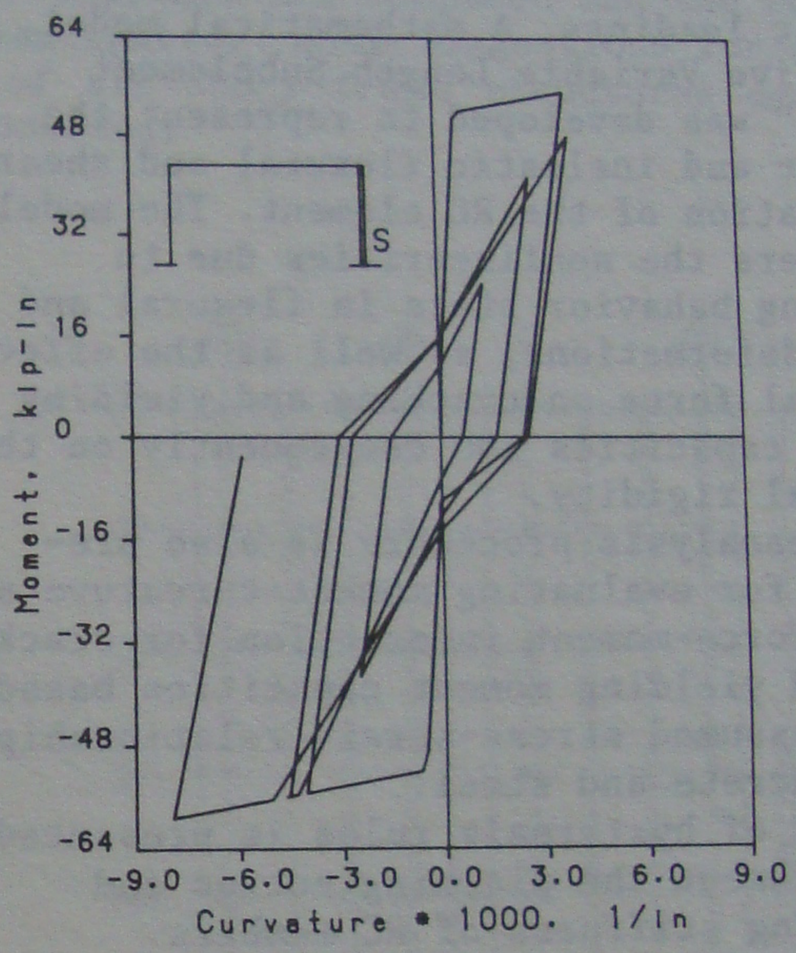

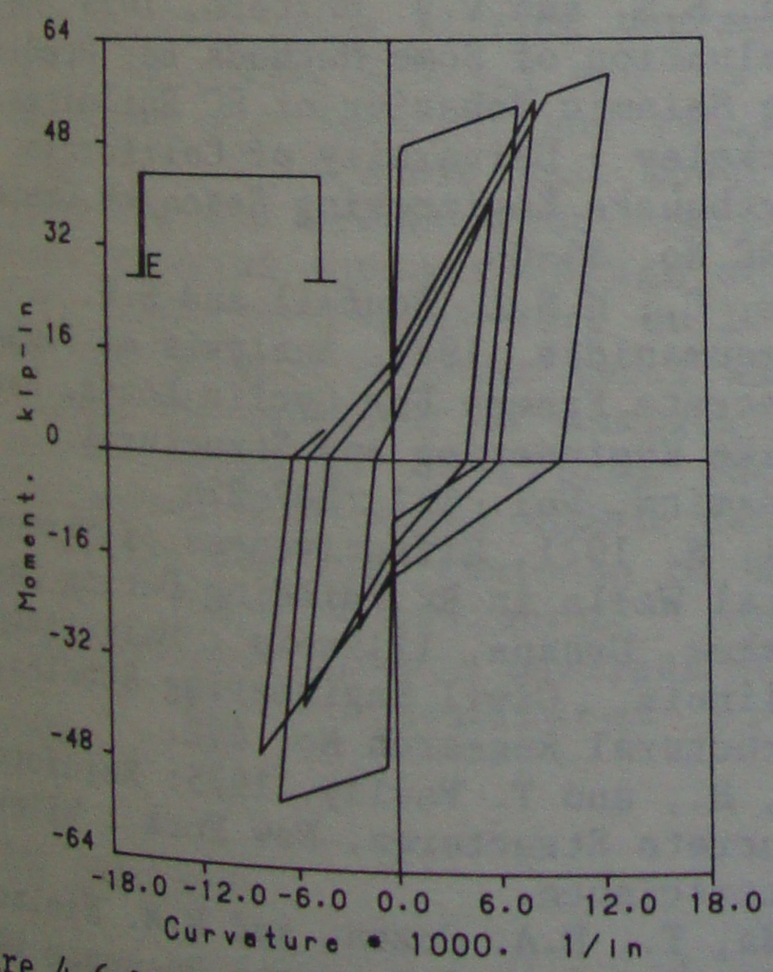

Figure 4.6 Moment-curvature at left column (a) cracking, (b) strain-hardening subelement (c) element end

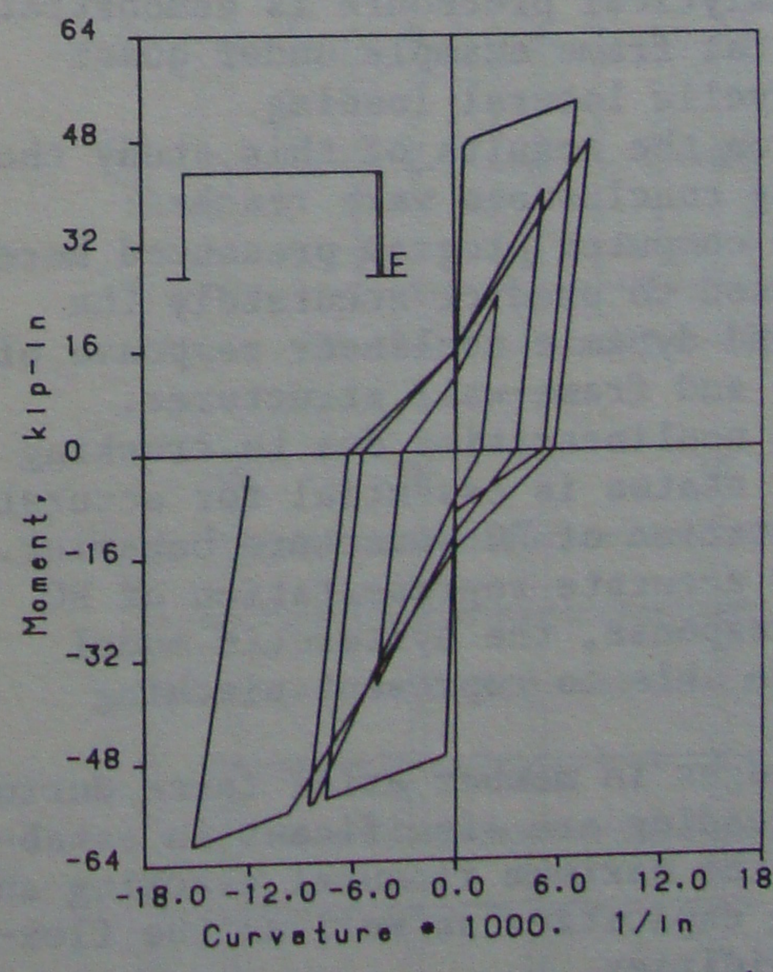

Figure 4.7 Moment-curvature at right column (a) cracking (b) strain-hardening subelement (c) element end

2. The effects of change in axial force due to the overturning moment on the cracking and moment capacities and flexural rigidities. This relation is significant when the hysterestic moment curvatures of the left and right columns are compared. The results obtained indicate a more rational nonlinear response analysis of the RC frame and frame-wall structures, and consequently a more accurate response analysis with the inclusion of inertia and damping forces.

5 SUMMARY AND CONCLUSION

The purpose of this paper was to provide an analytical procedure to evaluate the nonlinear response of RC frame and frame-wall structures subjected to static and/or dynamic loadings. A mathematical model, the "Five Variable Length Subelement Model," was developed to represent the elastic and inelastic flexural and shear deformation of the RC element. The model considers the nonlinearities due to cracking bahavior state in flexural and shear deformations, as well as the effect of axial force on cracking and yielding moment capacities and consequently on the flexural rigidity.

A preanalysis procedure is also presented for evaluating moment-curvature and axial force-moment interaction for cracking and yielding moment capacities based on an assumed stress-strain relationship for concrete and steel.

A set of hysteresis rules is presented to represent the pinching action and unloading stiffness of RC members.

The analytical procedure is demonstrated on a portal frame example under quasi-static cyclic lateral loading.

Based on the results of this study the following conclusions were reached:

1. The computer program presented here can be used to predict accurately the static and dynamic nonlinear response of RC frame and frame-wall structures.

2. The nonlinearities due to cracking behavior states is essential for accurate representation of RC structure behavior.

3. For accurate representation of RC member response, the hysteretic model should be able to represent pinching action.

4. Changes in member axial force during cyclic loading are significant in establishing the maximum flexural cracking and yielding capacities as well as the flexural rigidities.

REFERENCES

Aktan, A.E. and V.V. Bertero. 1984. Earthquate Response of a 1/5th-Scale Model of a 7-Story Reinforced Concrete Frame-Wall Structural System. San Francisco : 8th World Conference on Earthquake Engineering Vol. VI 651-658.

Giberson, M.F. 1967. The Response of Nonlinear Multistory Structures Subjected to Earthquake Excitation. Pasadena, California : Earthquake Engineering Research Laboratory and Institute of Technology.

Gulkan, P. and M. Sozen. 1971. Response and Energy Dissipation of Reinforced Concrete Frames Subjected to Strong Base Motion. Urbana, Illinois : University of Illinois. Structural Research Series No. 377.

Hashish, A.A. 1987. An Assessment of Damping and Strain-Rate Effects on the Nonlinear Response of RC Buildings Structures. Detroit, Michigan : Wayne State University, Civil Engineering Department, Ph.D. Dissertation.

Kaba, S.A. and S.A. Mahin. 1983. Interactive Computer Analysis Methods For Predicting The Inelastic Cyclic Behavior of Structural Sections. Berkeley, California : University of California. Earthquake Engineering Research Center, Report No. UCB/EERC-83/18, College of Engineering.

Keshavarzian, M. and W.C. Schnobirch. 1984. Computed Nonlinear Seismic Response of RC Wall-Frame Structures. Urbana, Illinois : University of Illinois, Civil Engineering Studies, Structural Research Series No. 515.

Mahin, S.A. and V.V. Bertero. 1975. An Evaluation of Some Methods for Predicting Seismic Behavior of RC Buildings. Berkeley : University of California. Earthquake Engineering Research Center, EERC No. 85-05.

Meyer, C., M.S.L. Roufail and S.G. Arzoumanidis. 1983. Analysis of Damaged Concrete Frames For Cyclic Loads. Earthquake Engineering and Structural Dynamics, Vol. 111 :207-228.

Otani, S. 1971. Effectiveness of Structural Walls in RC Building During Earthquakes. Urbana, Illinois : University of Illinois. Civil Engineering Studies, Structural Research No. 492.

Park, R., and T. Paulay. 1975: Reinforced Concrete Structures. New York : Wiley - Interscience.

Takeda, T., M.A. Sozen, and N.N. Nielsen. 1970. Reinforced Concrete Response to Simulated Earthquakes. J. of Struct. Div., ASCE :2557-2574.